New perspectives on cosmological shocks and magnetic fields in galaxy clusters

Christoph Pfrommer[1]

in collaboration with

Jonathan Dursi[2], Tom Jones[3]

[1]Heidelberg Intitute for Theoretical Studies, Germany
[2]Canadian Institute for Theoretical Astrophysics/SciNet Consortium, Canada
[3]University of Minnesota, Minneapolis, USA

Sep 30, 2010 / Stockholm University

Outline

1. Using a radio galaxy to probe an accretion shock
   - The jet of NGC 1265
   - A puzzling radio arc
   - Perseus accretion shock
2. Magnetic draping on spiral galaxies
   - Polarized radio ridges
   - Physics of magnetic draping
   - Draping and synchrotron emission
3. Implications and speculations
   - Magnetic field orientations
   - Kinetic plasma instabilities
   - Cosmological evolution of clusters

Total synchrotron intensity of NGC 1265

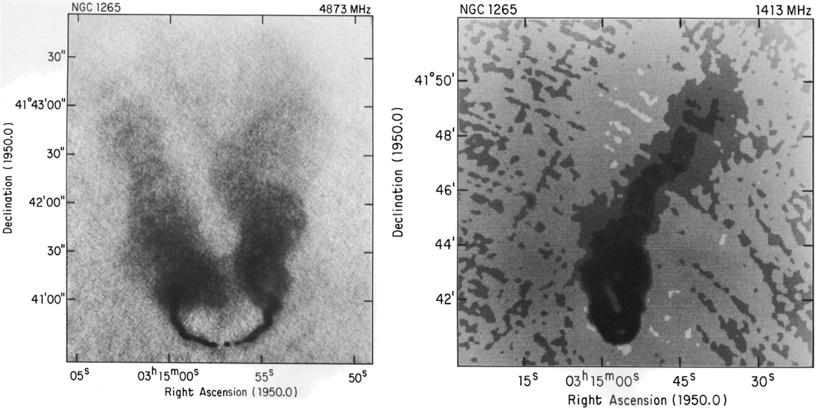

O'Dea & Owen (1986): small scale/high-resolution 4.9 GHz-image *(left)* and on large scales @ 1.4 GHz *(right)*

Simulating bipolar AGN jets in a turbulent ICM wind

Code: 3D MHD TVD with passive CR electrons

- simulation duration: 215 Myr
- tail length: $\sim$ 600 kpc
- jet power: 5×10^{44} erg/s
- $\mathcal{M}_{\text{jet}} = 3$ and $\mathcal{M}_{\text{wind}} = 1.5$
- jet radius $r_{\text{jet}} = 5$ kpc, $P_{\text{jet}} \sim P_{\text{icm}}$
- bending radius:

$$r_{\text{b}} \sim \left(\frac{\mathcal{M}_{\text{jet}}}{\mathcal{M}_{\text{wind}}}\right)^2 \frac{P_{\text{jet}}}{P_{\text{icm}}} r_{\text{jet}} \sim 20\,\text{kpc}$$

(credit to David Porter, Pete Mendygral, & Tom Jones)

Bipolar AGN jets in an ICM wind: magnetic field

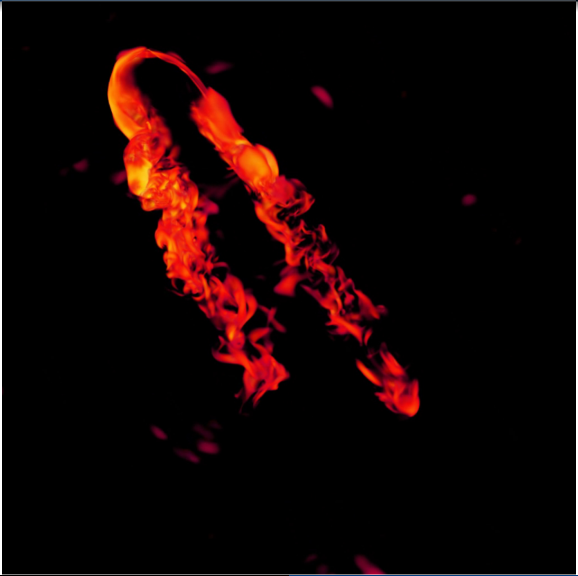

Bipolar AGN jets in an ICM wind: synthetic radio

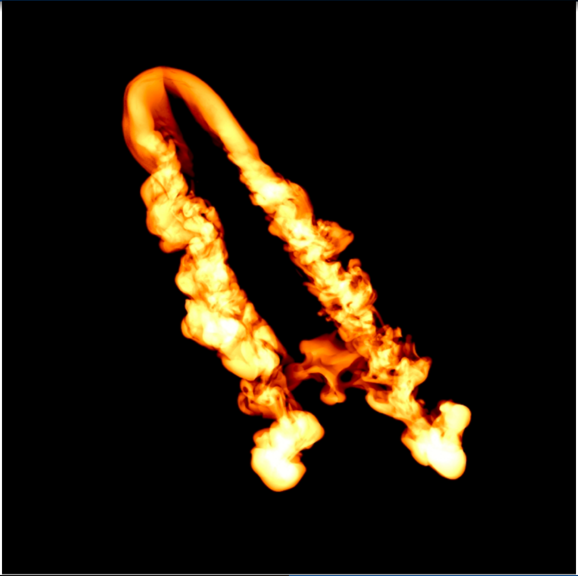

Radio properties of NGC 1265

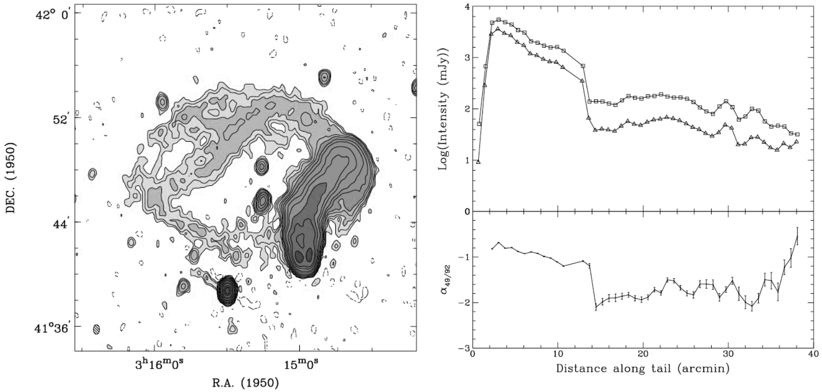

Sijbring & de Bruyn (1998), *left:* total radio brightness @ 600 MHz, $S_{600\,\mathrm{MHz}}$, of NGC 1265; *right:* variations of $S_{600\,\mathrm{MHz}}$ *(triangles)*, $S_{150\,\mathrm{MHz}}$ *(squares)* and spectral index *(bottom)* along the tail of NGC 1265

Previous models of NGC 1265 and why they fail

1. chance superposition of several independent head-tail galaxies
   → *lack of observed strong radio sources in this field*

Previous models of NGC 1265 and why they fail

1. chance superposition of several independent head-tail galaxies
   $\rightarrow$ *lack of observed strong radio sources in this field*
2. re-acceleration of electrons in the turbulent wake of a galaxy
   $\rightarrow$ *contrived projection probabilities and implausible energetics (re-acceleration efficiency* $\sim 3\%$*)*

Previous models of NGC 1265 and why they fail

1. chance superposition of several independent head-tail galaxies
$\rightarrow$ *lack of observed strong radio sources in this field*
2. re-acceleration of electrons in the turbulent wake of a galaxy
$\rightarrow$ *contrived projection probabilities and implausible energetics (re-acceleration efficiency* $\sim 3\%$*)*
3. ‘radio tail’ traces a helical cluster wind
$\rightarrow$ *wind needs special alignment with LOS, fine-tuned re-acceleration that balances electron cooling and avoids fanning out the well-confined radio emission along the arc*

Previous models of NGC 1265 and why they fail

1. chance superposition of several independent head-tail galaxies
$\rightarrow$ *lack of observed strong radio sources in this field*
2. re-acceleration of electrons in the turbulent wake of a galaxy
$\rightarrow$ *contrived projection probabilities and implausible energetics (re-acceleration efficiency* $\sim 3\%$*)*
3. ‘radio tail’ traces a helical cluster wind
$\rightarrow$ *wind needs special alignment with LOS, fine-tuned re-acceleration that balances electron cooling and avoids fanning out the well-confined radio emission along the arc*
4. ‘radio tail’ outlines ballistic orbit of NGC 1265
$\rightarrow$ *requires dark object with* $M \gtrsim M_{\mathrm{NGC\ 1265}} \simeq 3 \times 10^{12} M_{\odot}$ *orbiting the galaxy, no explanation of change of orbit and same challenges regarding electron cooling and re-acceleration*

Requirements for any model of NGC 1265

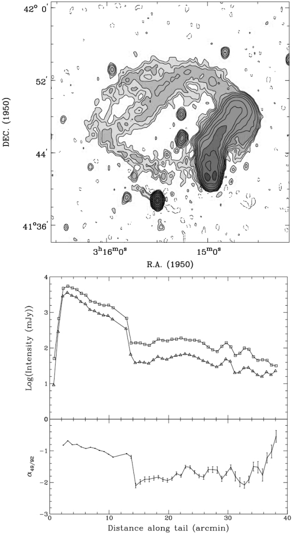

- bright narrow angle tail radio jet: synchrotron cooling
- transition region: change of winding direction and sharp drop in S_ν and α
- coherent properties along the dim radio ring, confined morphology

$\rightarrow$ *we are looking at 2 electron populations in projection possibly suggesting 2 different epochs of feedback:*

$\rightarrow$ active jet + detached radio bubble that recently got energized coherently across 300 kpc, potentially by a shock

Plasma bubble crosses shock and transforms to torus

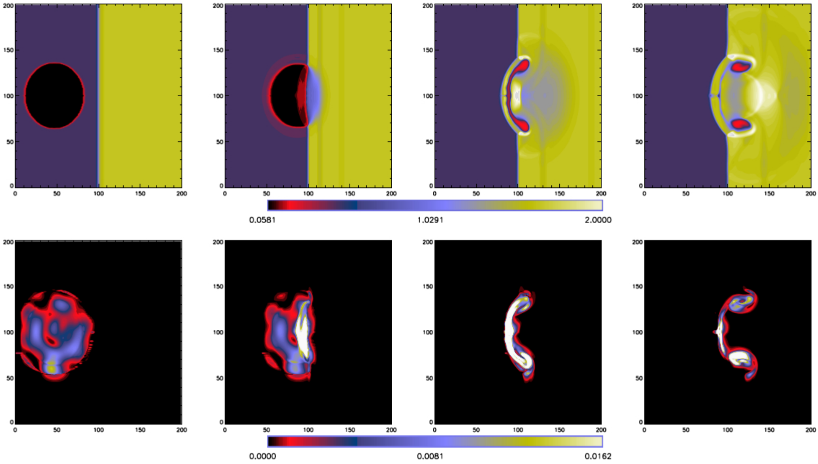

Enßlin & Brüggen (2002): gas density *(top)* and magnetic energy density *(bottom)*

Synthetic radio emission of shock-transformed bubble

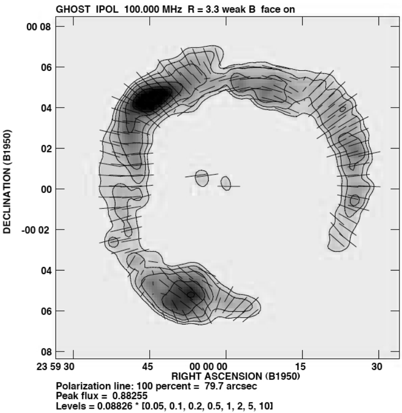

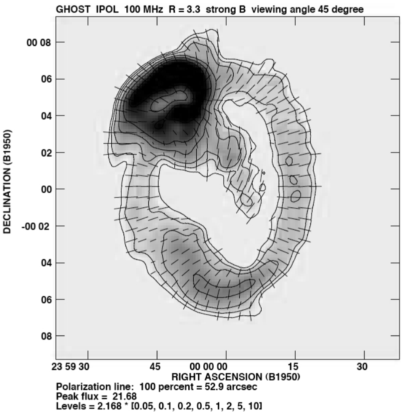

Enßlin & Brüggen (2002): total 100 MHz intensity and polarization E-vectors, strong shock/weak *B (left)* and strong shock/strong *B* model *(right)*

Cartoon of the time evolution of NGC 1265

C.P. & Jones (2010):

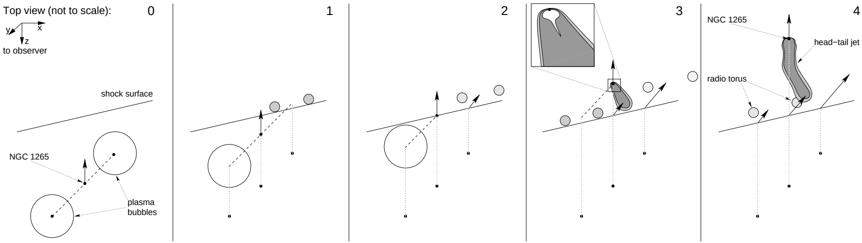

NGC 1265 as a perfect probe of a shock – 1

- galaxy velocity $\boldsymbol{v}$ not affected by shock $\rightarrow$ pre-shock conditions
- tail & torus as tracers of the post-shock flow
- conservation laws at oblique shock & extrapolating past orbits of head and tail $\rightarrow$ 3D model of NGC 1265:

$$
\begin{aligned}
\boldsymbol{v}_{2,\perp} &= \boldsymbol{v}_{1,\perp} = \boldsymbol{v} + v\cos\phi\,\boldsymbol{n}_\mathrm{s}, \\
\boldsymbol{v}_{2,\parallel} &= \frac{\boldsymbol{v}_{1,\parallel}}{C_\mathrm{s}} = -\frac{v}{C_\mathrm{s}}\cos\phi\,\boldsymbol{n}_\mathrm{s}, \\
\boldsymbol{v}_2 &= \boldsymbol{v} + v\cos\phi\,\frac{C_\mathrm{s}-1}{C_\mathrm{s}}\,\boldsymbol{n}_\mathrm{s},
\end{aligned}
$$

where $\boldsymbol{n}_\mathrm{s}$ is the shock normal, $C_\mathrm{s} = \rho_2/\rho_1$ the shock compression ratio, and $\phi = \arccos(-\boldsymbol{n}_\mathrm{s}\cdot\frac{\boldsymbol{v}}{v})$ is the 'shock obliquity'.

NGC 1265 as a perfect probe of a shock – 2

- conservation laws at oblique shock & extrapolating past orbits of head and tail → 3D model of NGC 1265:

$$\begin{aligned} v_{2,\mathrm{r}} &= \boldsymbol{e}_\mathrm{r} \cdot \boldsymbol{v}_2 = v_\mathrm{r} \left(1 - \frac{\cos\chi \cos\phi}{\cos\theta} \frac{C_\mathrm{s} - 1}{C_\mathrm{s}}\right), \\ v_{2,\mathrm{t}} &= \sqrt{(\boldsymbol{v}_2 - v_{2,\mathrm{r}} \boldsymbol{e}_\mathrm{r})^2} = \left[\frac{v_\mathrm{r}^2}{\cos^2\theta} \left(1 - \cos^2\phi \frac{C_\mathrm{s}^2 - 1}{C_\mathrm{s}^2}\right)\right. \\ &- \left. v_\mathrm{r}^2 \left(1 - \frac{\cos\chi \cos\phi}{\cos\theta} \frac{C_\mathrm{s} - 1}{C_\mathrm{s}}\right)^2\right]^{1/2}, \end{aligned}$$

where $\boldsymbol{e}_\mathrm{r}$ and $\boldsymbol{e}_\mathrm{t}$ are unit vectors along and transverse to the LOS,
$\chi = \arccos(\ \boldsymbol{e}_\mathrm{r} \cdot \boldsymbol{n}_\mathrm{s})$ is the 'shock orientation', and
$\theta = \arccos(-\boldsymbol{e}_\mathrm{r} \cdot \frac{\boldsymbol{v}}{v})$ the 'inclination of the galaxy's orbit'.

Derived geometry for NGC 1265

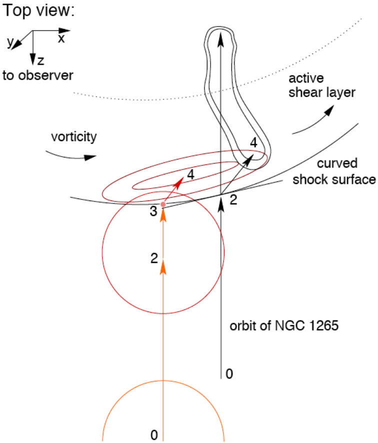

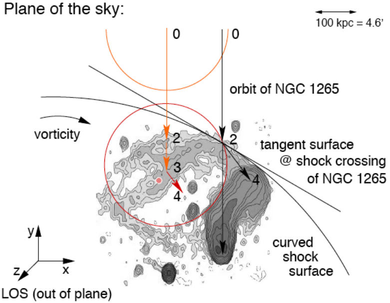

C.P. & Jones (2010)

Properties of the Perseus accretion shock

- Faraday rotation values and dispersion of the jet low and consistent with originating from the lobe → NGC 1265 on the near side of the cluster around the virial radius and shock likely generated by accretion!
- bubble compression factor:

$$C = \frac{V_{\rm bubble}}{V_{\rm torus}} = \frac{\frac{4}{3}\pi R^3}{2\pi^2 R r_{\rm min}^2} = \frac{2}{3\pi}\left(\frac{R}{r_{\rm min}}\right)^2 \simeq 6 - 10$$

  radio plasma is adiabatically compressed across the shock passage according to $P_2/P_1 = C^{\gamma_{\rm rel}}$, where $\gamma_{\rm rel} = 4/3$
- assuming that the radio bubble is in pressure equilibrium with its surroundings, we estimate the shock jumps:

$$\frac{P_2}{P_1} \simeq 21.5, \quad \frac{\rho_2}{\rho_1} \simeq 3.4, \quad \frac{T_2}{T_1} \simeq 6.3, \quad \text{and } \mathcal{M} \simeq 4.2$$

Limits on the infalling warm-hot intergalactic medium

extrapolating X-ray density and temperature profiles of Perseus to R_{200}, we can derive pre-shock values for ρ and T that reflect upper limits on the gas properties in the infalling warm-hot intergalactic medium:

$$
\begin{aligned}
kT_1 &\lesssim 0.4\,\mathrm{keV} \\
n_1 &\lesssim 5\times10^{-5}\,\mathrm{cm}^{-3} \\
P_1 &\lesssim 3.6\times10^{-14}\,\mathrm{erg\,cm}^{-3}
\end{aligned}
$$

Evidence for shear flows

- if ellipticity was due to projection of a ring-like torus $\rightarrow$ $\boldsymbol{n}_\mathrm{s}$ and $\boldsymbol{v}$ would not have EW components; momentum conservation at the oblique shock implies a post-shock deflection in the plane containing the LOS
$\rightarrow$ shear flow needed to explain the westward bending of the tail

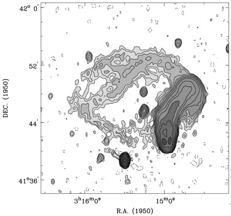

Evidence for shear flows

- if ellipticity was due to projection of a ring-like torus → $\boldsymbol{n}_\mathrm{s}$ and $\boldsymbol{v}$ would not have EW components; momentum conservation at the oblique shock implies a post-shock deflection in the plane containing the LOS
  → shear flow needed to explain the westward bending of the tail
- if the bending of the tail was due to oblique shock deflection, $\boldsymbol{n}_\mathrm{s}$ would have a component pointing westwards; projecting an intrinsically ring-like torus would yield an apparent ellipsoidal torus with the main axis at some angle with the EW direction on the plane of the sky
  → need shear flow that re-aligns the elliptical torus with the observed EW direction

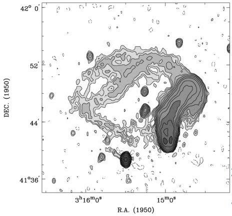

Evidence for shear flows

- if ellipticity was due to projection of a ring-like torus $\rightarrow$ $\boldsymbol{n}_\mathrm{s}$ and $\boldsymbol{v}$ would not have EW components; momentum conservation at the oblique shock implies a post-shock deflection in the plane containing the LOS $\rightarrow$ shear flow needed to explain the westward bending of the tail
- if the bending of the tail was due to oblique shock deflection, $\boldsymbol{n}_\mathrm{s}$ would have a component pointing westwards; projecting an intrinsically ring-like torus would yield an apparent ellipsoidal torus with the main axis at some angle with the EW direction on the plane of the sky $\rightarrow$ need shear flow that re-aligns the elliptical torus with the observed EW direction
- assuming that $\boldsymbol{n}_\mathrm{s} \parallel \nabla\Phi_\mathrm{Perseus}$ $\rightarrow$ implied shock curvature causes a post-shock vorticity that shears the gas westwards:

$$\frac{\varepsilon_\mathrm{shear}}{\varepsilon_\mathrm{th,2}} = \frac{\mu m_\mathrm{p} v_\perp^2}{3kT_2} \simeq 0.14,$$

with $kT_2 \simeq 2.4\,\mathrm{keV}$ and $v_\perp \simeq 400\,\mathrm{km/s}$.

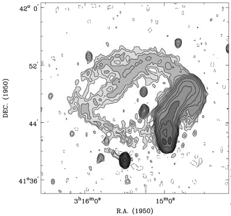

Conclusions on radio galaxies as probes of shocks

- consistent 3D model of NGC 1265
- prediction of a very interesting source class for LOFAR
- radio galaxies as perfect probes of pre- and post-shock flows:
    - hydrodynamic jumps and Mach numbers
    - statistical properties of the infalling WHIM (+ X-rays)
    - estimating the curvature radius of shocks and induced shear flows

$\rightarrow$ implications for intra-cluster turbulence as well as generation and amplification of large-scale magnetic fields!

Polarized synchrotron emission in a field spiral: M51

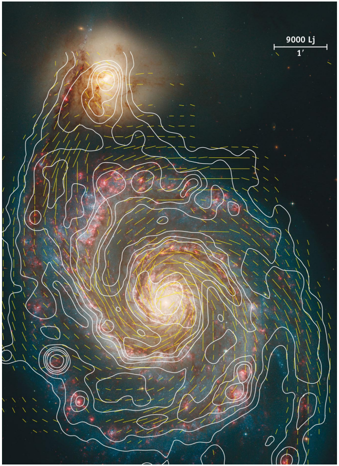

MPIfR Bonn and Hubble Heritage Team

- polarized synchrotron intensity follows the spiral pattern and is strongest in between the spiral arms (NGC 6946)
- the polarization 'B-vectors' are aligned with the spiral structure
- a promising generating mechanism is the *dynamo which transfers mechanical into magnetic energy* (Beck et al. 1996)

Ram-pressure stripping of cluster spirals

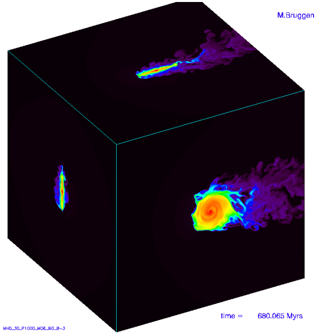

Brueggen (2008)

- 3D hydrodynamical simulations show that low-density gas in between spiral arms is quickly stripped irrespective of disk radius (Tonnesen & Bryan 2010)
- being flux-frozen into this dilute plasma, the large scale field will also be stripped, leaving behind the small scale field in the star forming regions

$\rightarrow$ beam depolarization effects and superposition of causally unconnected star forming patches along the line-of-sight cause the resulting radio synchrotron emission to be effectively unpolarized

Polarized synchrotron ridges in Virgo spirals

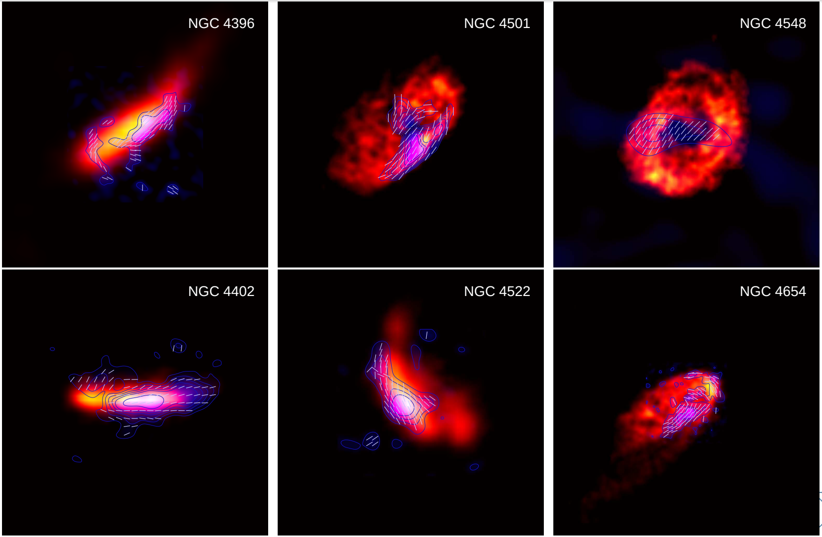

Vollmer et al. (2007): 6 cm PI (contours) + B-vectors; Chung et al. (2009): HI (red)

Draping field lines around a moving object

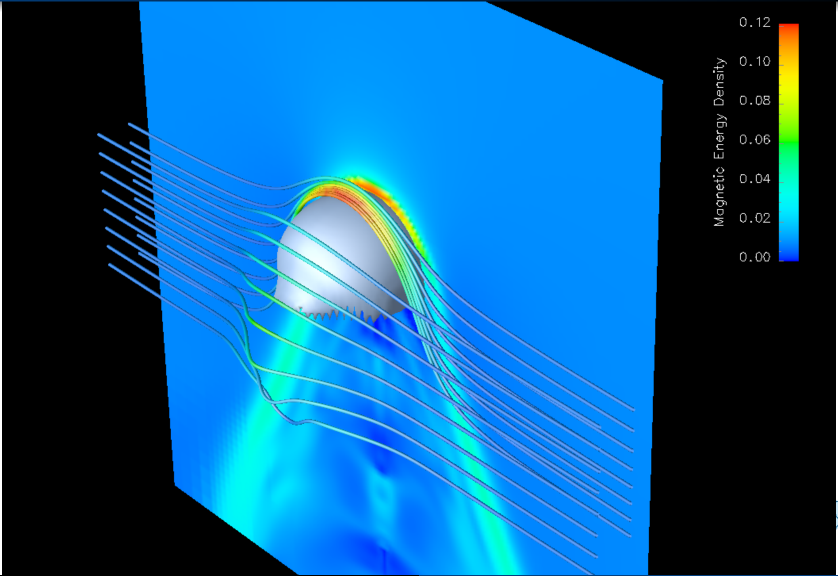

Draping of the interplanetary field over Venus

- Venus and Mars do not have a global magnetic field
- *right:* spatial distribution of the magnetic field strength in the plasma environment surrounding Venus (Venus Express)

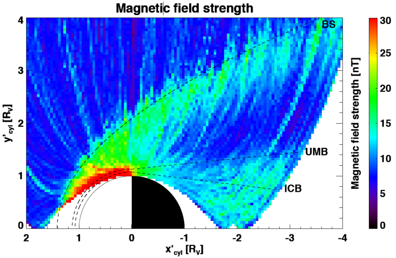

Guicking et al. (2010)

- draping of solar wind magnetic field around Venus/Mars leads to the formation of magnetic pile-up region and the magneto-tail $\rightarrow$ enhanced magnetic field strength in the planets' wake

Magnetic draping around a spiral galaxy – MHD

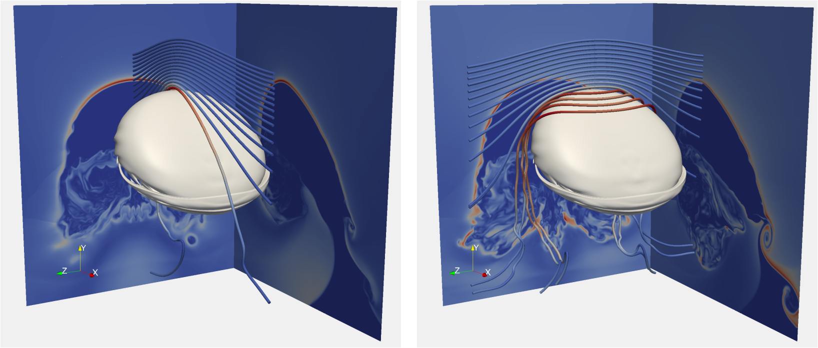

Athena simulations of spiral galaxies interacting with a uniform cluster magnetic field. There is a sheath of strong field draped around the leading edge (field strength is color coded).

Magnetic draping around a spiral galaxy – physics

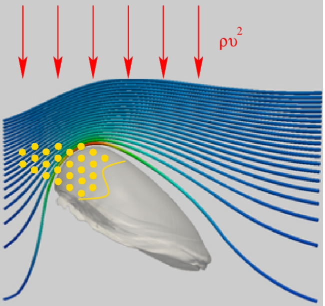

- the galactic ISM is pushed back by the ram pressure wind $\sim \rho\upsilon^2$
- the stars are largely unaffected and lead the gas
- the draping sheath is formed at the contact of ISM/ICM
- as stars become SN, their remnants accelerate CRes that populate the field lines in the draping layer

- CRes are transported diffusively (along field lines) and advectively as field lines slip over the galaxy
- CRes emit radio synchrotron radiation in the draped region, tracing out the field lines there $\rightarrow$ coherent polarized emission at the galaxies' leading edges

Magnetic draping and polarized synchrotron emission

Synchrotron B-vectors reflect the upstream orientation of cluster magnetic fields

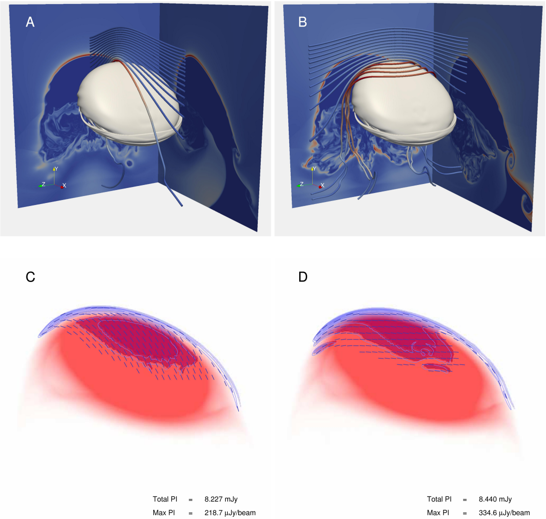

Simulated polarized synchrotron emission

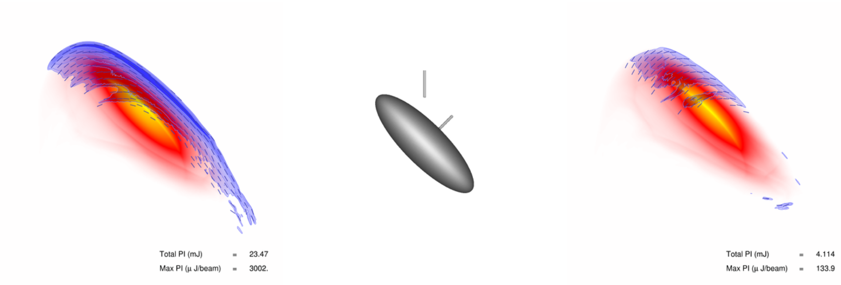

Movie of the simulated polarized synchrotron radiation viewed from various angles and with two field orientations.

Streamlines in the rest frame of the galaxy

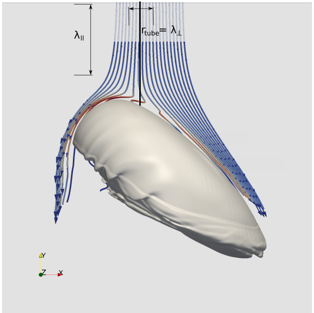

- as the flow approaches the galaxy it decelerates and gets deflected
- only those streamlines initially in a narrow tube of radius $\lambda_\perp \simeq R/\sqrt{3\beta\mathcal{M}^2} \simeq R/15 \simeq 1.3$ kpc from the stagnation line become part of the magnetic draping layer (color coded) $\rightarrow$ constraints on λ_B
- the streamlines that do not intersect the tube get deflected away from the galaxy, become never part of the drape and eventually get accelerated (Bernoulli effect)
- note the kink feature in some draping-layer field lines due to back reaction as the solution changes from the hydrodynamic potential flow solution to that in the draped layer

Magnetic draping of a non-uniform B-field

(Non-)observation of polarization twist constrains magnetic coherence length

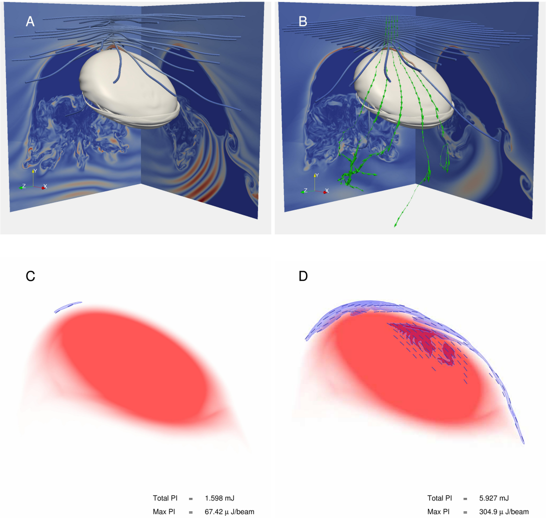

Magnetic coherence scale estimate by radio ridges

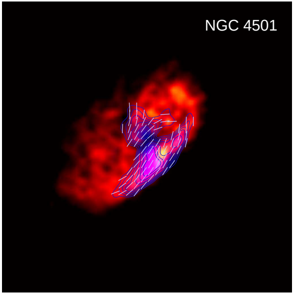

- observed polarised draping emission $\rightarrow$ field coherence length λ_B is at least galaxy-sized
- if $\lambda_B \sim 2R_{\rm gal}$, then the change of orientation of field vectors imprint as a change of the polarisation vectors along the vertical direction of the ridge showing a 'polarisation-twist'

- the reduced speed of the boundary flow means that a small $L_{\rm drape}$ corresponds to a larger length scale of the unperturbed magnetic field ahead of the galaxy NGC 4501

$$L_{\rm coh} \simeq \eta L_{\rm drape} v_{\rm gal}/v_{\rm drape} = \eta \tau_{\rm syn} v_{\rm gal} > 100\,{\rm kpc},$$

with $\tau_{\rm syn} \simeq 5 \times 10^7$ yr, $v_{\rm gal} \simeq 1000\,{\rm km/s}$, and a geometric factor $\eta \simeq 2$

Varying galaxy inclination and magnetic tilt

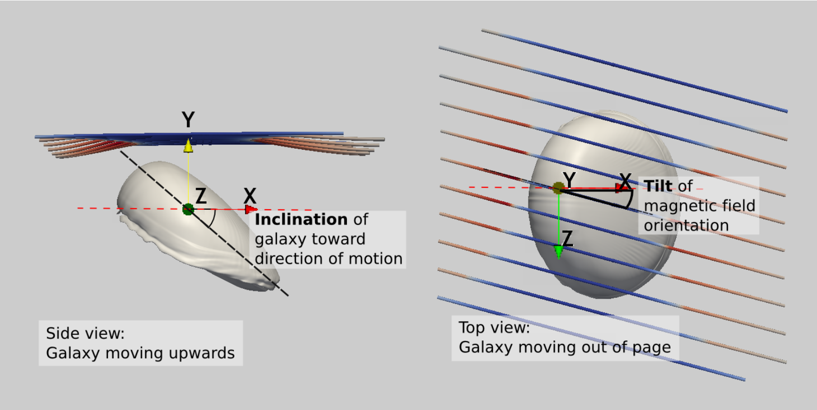

Observations versus simulations

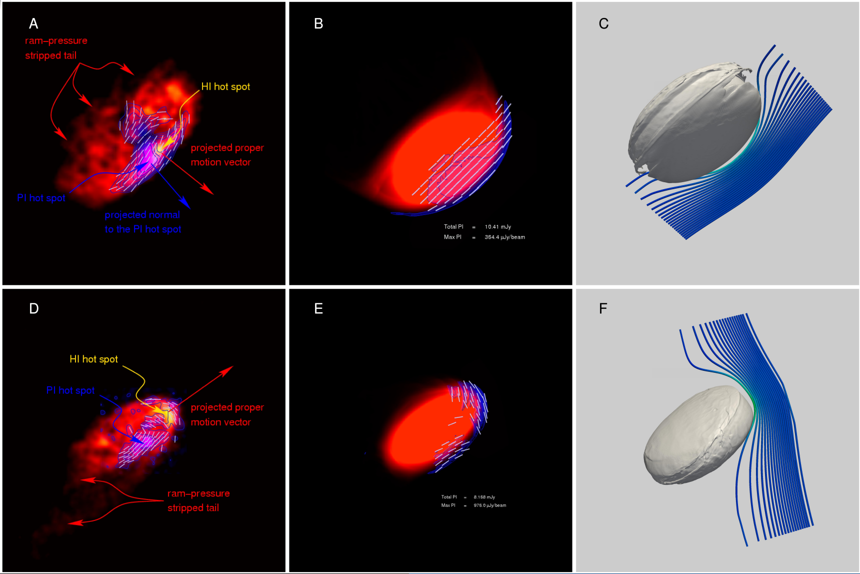

Biases in inferring the field orientation

- uncertainties in estimating the 3D velocity: v_r, ram-pressure stripped gas visible in HI morphology $\rightarrow \hat{\boldsymbol{v}}_\mathrm{t}$
- *direction-of-motion asymmetry:* magnetic field components in the direction of motion bias the location of $B_{\mathrm{max,\ drape}}$ (figure to the right): draping is absent if $\boldsymbol{B} \parallel \boldsymbol{v}_\mathrm{gal}$

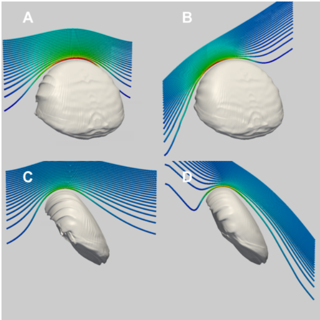

- *geometric bias:* polarized synchrotron emission only sensitive to traverse magnetic field B_t ($\perp$ to LOS) $\rightarrow$ maximum polarised intensity may bias the location of $B_{\mathrm{max,\ drape}}$ towards the location in the drape with large B_t

Mapping out the magnetic field in Virgo

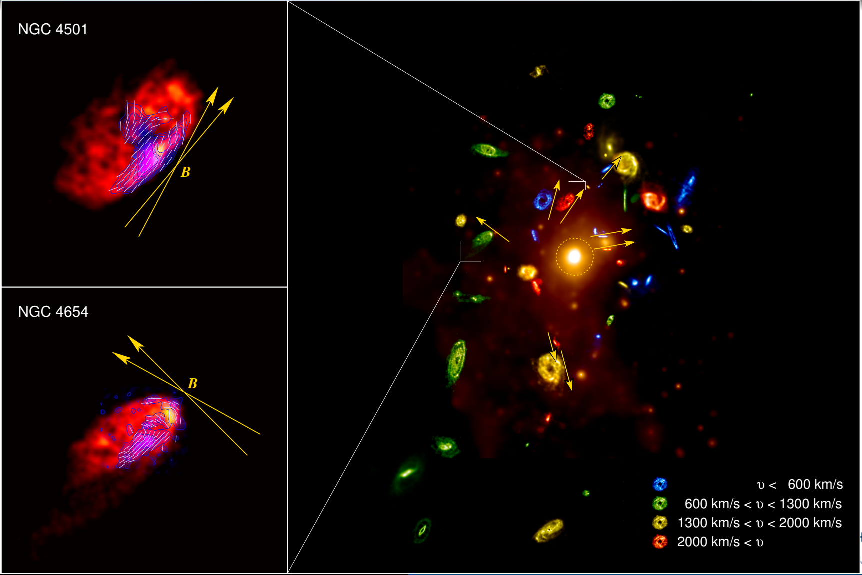

Magneto-thermal instability: the idea

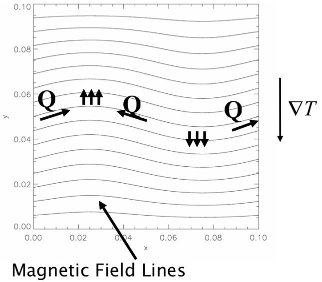

Figure from I. Parrish

Convective stability in a gravitational field:

- Classical Schwarzschild criterion: $\frac{\mathrm{d}S}{\mathrm{d}z} > 0$
- long MFP, Balbus criterion: $\frac{\mathrm{d}T}{\mathrm{d}z} > 0$
- new instability causes field lines to reorient radially → efficient thermal conduction radially (close to Spitzer)

The non-linear behavior of the MTI (Parrish & Stone 2007).

- Adiabatic boundary conditions for $T(r)$: the instability can exhaust the source of free energy → isothermal profile
- Fixed boundary conditions for $T(r)$: field lines stay preferentially radially aligned (35 deg mean deviation from radial)

Magneto-thermal instability: the idea

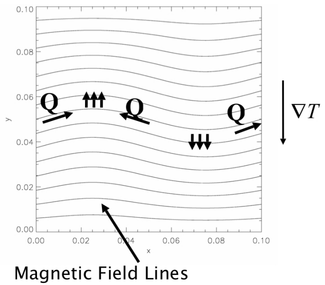

Figure from I. Parrish

Convective stability in a gravitational field:

- Classical Schwarzschild criterion: $\frac{\mathrm{d}S}{\mathrm{d}z} > 0$
- long MFP, Balbus criterion: $\frac{\mathrm{d}T}{\mathrm{d}z} > 0$
- new instability causes field lines to reorient radially $\rightarrow$ efficient thermal conduction radially (close to Spitzer)

The non-linear behavior of the MTI (Parrish & Stone 2007).

- Adiabatic boundary conditions for $T(r)$: the instability can exhaust the source of free energy $\rightarrow$ isothermal profile
- Fixed boundary conditions for $T(r)$: field lines stay preferentially radially aligned (35 deg mean deviation from radial)

Gravitational shock wave heating

The observed temperature profile in clusters is decreasing outwards which is the necessary condition for MTI to operate → *gravitational heating can stabilize the temperature profile:*

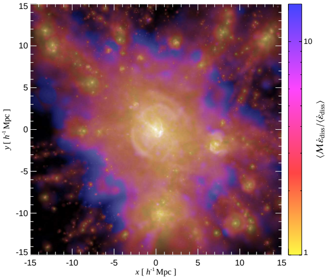

Mach number distribution weighted by $\varepsilon_{\text{diss}}$.

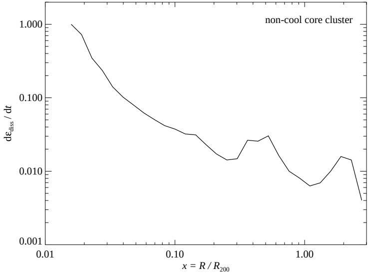

Energy flux through shock surface $\dot{E}_{\text{diss}}/R^2 \sim \rho \upsilon^3 \rightarrow$ increase towards the center

Implications for thermal stability of galaxy clusters

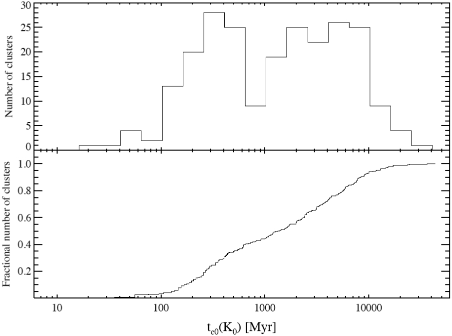

Cavagnolo et al. (2009)

- radial fields in non-cool core clusters (NCCs) imply efficient thermal conduction that stabilizes these systems against entering a cool-core state: $\tau_{\mathrm{cond}} = \lambda^2/\chi_{\mathrm{C}} \simeq 2.3 \times 10^7\,\mathrm{yr}\,(\lambda/100\,\mathrm{kpc})^2$, where χ_{C} is the Spitzer thermal diffusivity (using $kT = 10\,\mathrm{keV}$, $n = 5 \times 10^{-3}\,\mathrm{cm}^{-3}$)
- current cosmological cluster simulations fail to reproduce NCCs that have no AGN activity $\rightarrow$ MHD + anisotropic conduction

Speculation: evolutionary sequence of galaxy clusters

- After a merging event of a non-cool core cluster, the injected turbulence decays on an eddy turnover time $\tau_\mathrm{eddy} \simeq L_\mathrm{eddy}/\upsilon_\mathrm{turb} \sim 300\,\mathrm{kpc}/(300\,\mathrm{km/s}) \sim 1$ Gyr.
- The magneto-thermal instability grows on a similar timescale of less than 1 Gyr and the magnetic field becomes radially oriented.
- The efficient thermal conduction stabilizes this cluster until a cooling instability in the center may cause the cluster to enter a cooling core state – similar to Virgo now – and requires possibly feedback by an active galactic nuclei to be stabilized.

Magnetic draping at spiral galaxies in the Virgo cluster

nature physics

ARTICLES

PUBLISHED ONLINE: 16 MAY 2010 | DOI: 10.1038/NPHYS1657

Detecting the orientation of magnetic fields in galaxy clusters

Christoph Pfrommer[1]* and L. Jonathan Dursi[1,2]

Clusters of galaxies, filled with hot magnetized plasma, are the largest bound objects in existence and an important touchstone in understanding the formation of structures in our Universe. In such clusters, thermal conduction follows field lines, so magnetic fields strongly shape the cluster's thermal history; that some have not since cooled and collapsed is a mystery. In a seemingly unrelated puzzle, recent observations of Virgo cluster spiral galaxies imply ridges of strong, coherent magnetic fields offset from their centre. Here we demonstrate, using three-dimensional magnetohydrodynamical simulations, that such ridges are easily explained by galaxies sweeping up field lines as they orbit inside the cluster. This magnetic drape is then lit up with cosmic rays from the galaxies' stars, generating coherent polarized emission at the galaxies' leading edges. This immediately presents a technique for probing local orientations and characteristic length scales of cluster magnetic fields. The first application of this technique, mapping the field of the Virgo cluster, gives a startling result: outside a central region, the magnetic field is preferentially oriented radially as predicted by the magnetothermal instability. Our results strongly suggest a mechanism for maintaining some clusters in a 'non-cooling-core' state.

Conclusions on magnetic draping around galaxies

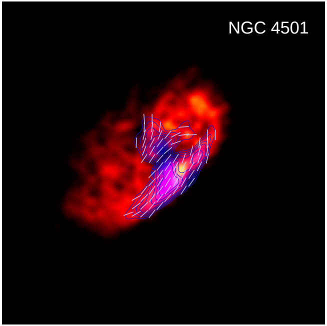

- draping of cluster magnetic fields naturally explains polarization ridges at Virgo spirals

Conclusions on magnetic draping around galaxies

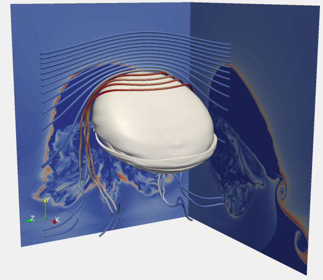

- draping of cluster magnetic fields naturally explains polarization ridges at Virgo spirals
- this represents a new tool for measuring the in situ orientation and coherence scale of cluster magnetic fields

Conclusions on magnetic draping around galaxies

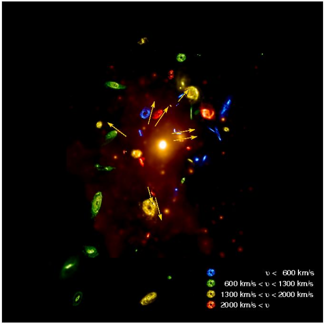

- draping of cluster magnetic fields naturally explains polarization ridges at Virgo spirals
- this represents a new tool for measuring the in situ orientation and coherence scale of cluster magnetic fields
- application to the Virgo cluster shows that the magnetic field is preferentially aligned radially

Conclusions on magnetic draping around galaxies

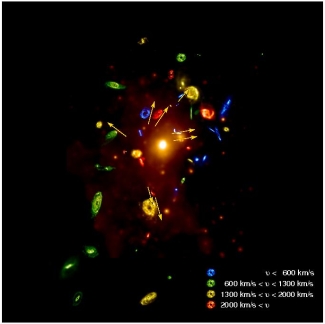

- draping of cluster magnetic fields naturally explains polarization ridges at Virgo spirals
- this represents a new tool for measuring the in situ orientation and coherence scale of cluster magnetic fields
- application to the Virgo cluster shows that the magnetic field is preferentially aligned radially

- this finding is suggestive that the MTI may be operating and implies efficient thermal conduction close to the Spitzer value
- it also proposes that non-cool core clusters are stabilized by thermal conduction

Literature for the talk

- Pfrommer & Jones, ApJ submitted, `arXiv:1004.3540`, *Radio galaxy NGC 1265 unveils the accretion shock onto the Perseus galaxy cluster*
- Pfrommer & Dursi, 2010, Nature Phys., 6, 520, *Detecting the orientation of magnetic fields in galaxy clusters*
- Dursi & Pfrommer, 2008, ApJ, 677, 993, *Draping of cluster magnetic fields over bullets and bubbles - morphology and dynamic effects*